

Papers published in *Hydrology and Earth System Sciences Discussions* are under open-access review for the journal *Hydrology and Earth System Sciences*

# Applied tracers for the observation of subsurface stormflow at the hillslope scale

J. Wienhöfer<sup>1,2</sup>, K. Germer<sup>3</sup>, F. Lindenmaier<sup>1</sup>, A. Färber<sup>3</sup>, and E. Zehe<sup>1</sup>

<sup>1</sup>Institute of Water and Environment, Technische Universität München, München, Germany

<sup>2</sup>Institute of Geoecology, University of Potsdam, Potsdam, Germany

<sup>3</sup>Institute of Hydraulic Engineering, Universität Stuttgart, Stuttgart, Germany

Received: 8 March 2009 – Accepted: 18 March 2009 – Published: 1 April 2009

Correspondence to: J. Wienhöfer (j.wienhoefer@bv.tu-muenchen.de)

Published by Copernicus Publications on behalf of the European Geosciences Union.

2961

## Abstract

Rainfall-runoff response in temperate humid headwater catchments is mainly controlled by hydrological processes at the hillslope scale. Applied tracer experiments with fluorescent dye and salt tracers are well known tools in groundwater studies at the large scale and vadose zone studies at the plot scale, where they provide a means to characterise subsurface flow. We extend this approach to the hillslope scale to investigate saturated and unsaturated flow paths concertedly at a forested hillslope in the Austrian Alps. Dye staining experiments at the plot scale revealed that cracks and soil pipes function as preferential flow paths in the fine-textured soils of the study area, and these preferential flow structures were active in fast subsurface transport of tracers at the hillslope scale. Breakthrough curves obtained under steady flow conditions could be fitted well to a one-dimensional convection-dispersion model. Under natural rainfall a positive correlation of tracer concentrations to the transient flows was observed. The results of this study demonstrate qualitative and quantitative effects of preferential flow features on subsurface stormflow in a temperate humid headwater catchment. It turns out that, at the hillslope scale, the interactions of structures and processes are intrinsically complex, which implies that attempts to model such a hillslope satisfactorily require detailed investigations of effective structures and parameters at the scale of interest.

## 1 Introduction

Understanding hydrological processes and runoff generation is of prime importance for hydrological predictions. Hillslopes act in many landscapes as “filters” for water to enter the stream or the deeper subsurface. Rainfall-runoff processes at this scale are intrinsically complex (Bonell, 1993; Williams et al., 2002). Hillslope geometry, soil and bedrock properties, the vegetation pattern, and rainfall characteristics crucially determine time scales and processes that dominate the rainfall runoff response. Especially

et al., 2002). Since Flury et al. (1994) dye staining techniques have become popular to visualise preferential flow pathways in excavated soil profiles at the plot scale (e.g. Blume et al., 2008; Weiler and Naef, 2003; Zehe and Flüher, 2001a), and also at the hillslope scale (Anderson et al., 2008; Noguchi et al., 1999). The advantage of dye staining experiments is that flow patterns can be obtained in high spatial resolution by image analysis. The major drawback of the method is that it is inherently invasive and destructive and thus limited in its applicability.

Besides dyes, salt tracers as bromide or chloride have been established to investigate flow and leaching processes in the vadose zone in soil column experiments (e.g. Binley et al., 1996; Jensen et al., 1996; Henderson et al., 1996), at the plot or lysimeter scale (e.g. Hornberger et al., 1990; Tsuboyama et al., 1994; Deeks et al., 2008) and at the field or hillslope scale (e.g. Roth et al., 1991; Lange et al., 1996; Zehe and Flüher, 2001b). Advantages of salt tracers are that they are non-sorptive and conservative. In contrast, their specific determination involves laborious sampling procedures and chromatography to obtain accurate concentrations.

too general  
specify which  
salts behave  
conservative

## 1.2 Outline of the paper: approach and objectives

This study comprises experimental work with different artificial tracers at different scales. At the hillslope scale, we employed fluorescent dyes and conservative salt tracers together with rainfall simulation experiments in order to investigate the hydrological functioning of the hillslope under quasi-steady state conditions and under transient (natural) rainfall conditions based on continuous concentration time series. To better understand the transport of these tracers in the specific soil material, we performed similar tracer tests on an undisturbed soil block from the studied hillslope. At the plot scale, we performed dye staining experiments using Brilliant Blue FCF to explore occurrence and type of subsurface flow paths.

The major objective of this study is to qualitatively and quantitatively assess possible subsurface flow paths and their functional role in hydraulic processes under heavy rainfall conditions. The experimental work aims at a better understanding of the processes

2965

and structures that are causing the fast reactions in spring discharge in the south west part of the Heums slope, which is deemed to be a critical source area for the slope movement. A specific objective is to test a lumped-parameter approach for an effective description of the system. A methodological objective is to test the feasibility of applied tracer tests associated with rainfall simulation in a steep forested environment with cohesive soils, with particular emphasis on the applicability of fluorescent dye tracers and in situ fluorimetry to investigate the interactions of the unsaturated and saturated zone processes. Before we describe the experimental setup, the employed tracers and the methods to analyse the tracer data in detail, we give a short description of the study site.

HEUMS

## 2 Materials and methods

### 2.1 Study area

The Heumös slope is located in the Vorarlberg Alps (Austria), 10 km south-east of the city of Dornbirn and 0.5 km south of the village of Ebnit (47° 21'0.2" N, 9° 44'46.6" E). A short overview is given here; further details on the site are given by Lindenmaier et al. (2005), Lindenmaier (2008) and Wienhöfer et al. (2009). The extension of the slope is 1800 m in east-west and about 500 m in a north-south direction; the elevation ranges from 940 to 1360 m. The Heumös slope belongs to the head of a steep mountainous catchment which is drained by the Ebnit/Dornbirn River. The long-term average annual precipitation depth is 2155 mm. The summer months (April to September) are the wetter season of the year, with average monthly rainfall depths between 160 and 250 mm and intensities of up to 12 mm in 10 min. The most extreme storm in the 100 year record occurred on 22–23 August 2005 and delivered 248.2 mm of rainfall in 37.7 h (Lindenmaier, 2008). Mean annual temperature is around 7°C; annual evapotranspiration is about 500–600 mm.

This study is focused on the source area of a spring (Fig. 1) in the south-western part

M.A.S.L.

Tiny  
and the

2966

Land  
is up

W accumulates to  
is up

of Heumös slope, which shows fast reactions to rainfall and is considered a source area of subsurface flow processes that trigger slope movement. It is a subcatchment of approximately 1000 m<sup>2</sup> delimited by two small ridges on the steep side slopes of the catchment, where vegetation is dominated by common spruce (*Picea abies*) and sycamore (*Acer pseudoplatanus*). Slope angles vary between 18 and 54° (median: 30°). Spring discharge is recorded in intervals of 10 min (water stage recorder: ATP15 Beaver, AquITronic Umweltmesstechnik GmbH, Kirchheim/Teck, Germany) and ranges from 0.02 to 0.33 l s<sup>-1</sup> and shows quick response to rainfall (Lindenmaier, 2008). The bedrock is built up by upper cretaceous sediments, mainly marls and limy marls. Soils are siltic and vertic Cambisols in the midslope, and stagnic and gleyic Cambisols and Gleysols at the hillslope toe. Soil depths vary between 0.35 m to >1.00 m (median 0.74 m); soil depth appears to be controlled by microrelief rather than by position along the slope line. Porosities in the topsoil (0–10 cm) are high (0.48–0.73, median 0.58) with low bulk densities (0.5–1.1 g cm<sup>-3</sup>, median 0.63 g cm<sup>-3</sup>), soil texture is sandy loam. Below a depth of 10 cm soil textures are significantly finer and classified as silt loam and silty clay loam. In situ measurements using a compact constant head permeameter (Amoozegar, 1989) indicate a decrease in saturated hydraulic conductivity with depth, from median values of 2.5 × 10<sup>-5</sup> m s<sup>-1</sup> in 12.5 cm and 1.3 × 10<sup>-5</sup> m s<sup>-1</sup> in 19–25 cm, respectively, to the range of 10<sup>-6</sup> to 10<sup>-7</sup> m s<sup>-1</sup> in 30–100 cm depth (Wienhöfer et al., 2009). At one-fifth of the measurement locations (*n*=41), regardless of measurement depth, the device's maximum measurable outflow rate of approximately 1 × 10<sup>-4</sup> m s<sup>-1</sup> (Sobieraj et al., 2004) was exceeded due to fast flow because of macropores.

V of  
better:  
Sycamore maple

## 2.2 Fluorescent dye and salt tracers

In the tracer experiments described in the following sections, the fluorescent dyes uranine (sodium fluorescein, CAS 518-47-8, C.I. 45350) and sulforhodamine G (CAS 5873-16-5, C.I. 45220) as well as the salt tracers sodium chloride (NaCl, CAS 7647-14-5) and sodium bromide (NaBr, CAS 7647-15-6) were used. Each of the tracer experiments presented in this paper consisted of three phases: (1) pre-saturation, (2)

2967

tracer application, and (3) flushing with tracer-free water. Tracers were applied manually in solvated form as pulse input onto the undisturbed soil surface from which only large pieces of litter were removed carefully by hand. Fluorescent dye tracer concentrations in the outflow were monitored in situ using fiber-optic fluorimeters (Mobiles LLF, Hermes Messtechnik, Stuttgart, Germany); for a description of the principle of fiber-optic fluorimetry see Ptak and Schmid (1996). Determination of salt concentrations was either done in situ with measurements of specific electrical conductivity, which were calibrated against salt concentrations, or with ion exchange chromatography on collected samples.

## 2.3 Soil block laboratory experiments

To quantify the interactions of fluorescence tracers and the soil material, an undisturbed soil block (surface area 0.25 × 0.25 m, depth 0.35 m) was isolated next to plot IIIb after the hillslope tracer tests. The block was surrounded by a wooden box and the voids filled with gypsum (cf. Bouma and Dekker, 1981). The edges along the surface were additionally covered with gypsum to minimise boundary effects, resulting in an uncovered surface area of 0.22 × 0.23 m. After the gypsum dried up, the soil block was carefully cut off at the base and transported to the laboratory, where it was mounted on a perforated metal plate over a plastic funnel. Tap water delivered from a constant head tank was used for infiltration; rates were chosen such that the whole soil surface was covered by a water film while ponding on the irregular soil surface was 5 mm or less. The tracers uranine and NaCl were applied in two runs each; details of the tracer application are given in Table 1. Dye tracer concentrations in the outflow were measured with a fluorimeter in intervals of 10 to 60 s. Salt tracer concentrations in the outflow were measured at one minute intervals using a hand-held conductivity-meter (Cond340i, WTW Wissenschaftlich-Technische Werkstätten GmbH, Weilheim, Germany). The pH of the outflow was checked on selected samples taken during the experiment. Flow was interrupted for 19 d during the first uranine transport experiment to check for non-ideal transport behaviour (Brusseau et al., 1997).

2968

## 2.4 Hillslope tracer experiments

Two sets of tracer experiments were conducted at the study site. Rainfall was simulated on four plots (total area: 106 m<sup>2</sup>) along the slope line (Fig. 1) with the use of oscillating sprinklers, as suggested by Zehe and Flüher (2001a). The sprinkling water was taken from a creek, approx. 100 m north of the spring. The sprinklers were fed from a storage container using two groundwater pumps (MP1, Grundfos, Bjerringbro, Denmark). The pumps and sprinklers were regulated to obtain a constant sprinkling rate of 12 mm h<sup>-1</sup> on all four plots. Rates of applied and natural rainfall were checked using tipping-bucket rain gauges and rainfall collectors.

### 2.4.1 First hillslope tracer experiment

The dyes uranine and sulforhodamine G and the salt tracers sodium bromide (NaBr) and sodium chloride (NaCl) were used for this experiment in August 2006. Sodium chloride was applied as a pulse from a line source (2.4×0.1 m, 0.2 m deep). The rest of the tracers were applied as a pulse onto the forest floor using a watering can. Tracers were applied subsequently on plots IV-I (cf. Table 1) at 10 min intervals. Sulforhodamine G concentrations were measured in the outflow from the cut-bank and uranine concentrations were measured in spring discharge; measurement intervals were 120 s. Salt concentrations were determined with ion exchange chromatography in the laboratory on selected samples from the spring. Samples were taken with an automatic sampling device (6700 Portable Sampler, Teledyne Isco Inc., Lincoln, NE, USA) in increasing intervals of 10 min to 60 min. Electrical conductivity and temperature were monitored at five-minute intervals at the spring (YSI 600 R, YSI Environmental, Yellow Springs, OH, USA).

IV to I

2969

### 2.4.2 Second hillslope tracer experiment

For this experiment in August 2007 the tracers uranine and sodium chloride were used. The tracers were applied as a pulse onto the forest floor using a watering can; the procedure was repeated for a second run of the experiment (for details on tracer application see Table 1). Uranine concentrations were measured in the outflow from the cut-bank near the hiking trail and in spring discharge at intervals of 10 s. At the cut-bank, a Thompson weir with a pressure transducer was installed to quantify discharge for the duration of this experiment. Electrical conductivity and temperature of the outflow were recorded at one-minute intervals using a hand-held conductivity-meter (Cond340i, WTW Wissenschaftlich-Technische Werkstätten GmbH, Weilheim, Germany). At the spring, a conductivity-meter (YSI 600 R, YSI Environmental, Yellow Springs, OH, USA) was used to record electrical conductivity and temperature of spring water at five-minute intervals.

## 2.5 Dye staining experiments

To qualitatively assess possible flow paths on the hillslope, we conducted three staining dye tracer experiments using Brilliant Blue FCF (CAS [3844-45-9], C.I. 42090). The location of the plots BB1-BB3 are shown in Fig. 1. Volumetric soil moisture was determined next to the plots BB1 (31 July 2006) and for BB2 (12 June 2007) with time domain reflectometry, and was about 0.18–0.2 and 0.45–0.55, respectively. The 14 days antecedent precipitation sum before application was 60.6, 89.0 and 175.2 mm for BB1, BB2 and BB3, respectively. The plots BB1 and BB3 received additional precipitation during the day before excavation (BB1: 21.0 mm, BB3: 2.8 mm). Brilliant Blue was applied in quantities of 20, 40 and 30 l, with a concentration of 4 g l<sup>-1</sup> to the plots BB1 (1 m<sup>2</sup>), BB2 (2 m<sup>2</sup>) and BB3 (1 m<sup>2</sup>), respectively. Application of tracer solution and additional water complies with input rates of 150 mm h<sup>-1</sup>. Soil profiles were excavated in horizontal and vertical layers the following day and photographs of the dye patterns under a 10 cm grid scale were taken with a digital camera. The images were

2970

analysed after Zehe and Flüher (2001a) and Blume et al. (2008), including rectification of the image, adjusting the tone curves to increase the contrast between stained and non-stained areas and computing a binary representation of the picture that allows determination of percent dye coverage.

## 5 2.6 Data manipulation and analysis

### 2.6.1 Estimation of tracer concentrations and treatment of time series

The time series of tracer signals (both fluorimeter and conductivity meter) and discharges were smoothed using a moving median function and turned to regular series in one minute values by taking each minute's median (tracer data) or linear interpolation (discharge data), except for the first hillslope tracer experiment where the fluorimeter measurement intervals of 120 s were used as a time base for all series. Calibrations were conducted in situ for each fluorimeter before and after each experiment. The calibrations resulted in linear relationships of signal and tracer concentrations in the range of 0–1000  $\mu\text{g l}^{-1}$  ( $r^2 > 0.99$ ). Background signals were subtracted from fluorimeter readings before determining fluorescence tracer concentrations. To determine salt tracer concentrations from conductivity meter readings, we calibrated the increase in electrical conductivity against concentrations of the applied salt tracer. The background conductivity, which was determined under rainfall simulation conditions before salt tracer was introduced into the system, was subtracted from the measured conductivity readings. Calibrations resulted in linear relationships of electrical conductivity and salt concentration in the range of 0–4  $\text{g l}^{-1}$  ( $r^2 > 0.99$ ).

### 2.6.2 Transfer function approach

For analysis of tracer breakthrough curves (BTCs), we adopted the transfer function approach, which is based on the probability density function (PDF) of the tracer travel times  $t$  along the transport distances (see Jury and Roth, 1990). In the case of a

1 uf

2971

nonreactive solute added as a narrow pulse to a system under steady-state water flow, the travel time PDF,  $f^f(l, t)$ , is equal to the normalised outflow flux concentration,  $C^f(l, t)$ , and is defined as

$$f^f(l, t) = \frac{C^f(l, t)}{\int_0^{\infty} C^f(l, \tau) d\tau} \quad (1)$$

To construct the travel time PDFs, mass fluxes  $C^f(l, t)$  [ $\text{g s}^{-1}$ ] were determined by multiplying effluent tracer concentration [ $\text{g l}^{-1}$ ] and discharge [ $\text{l s}^{-1}$ ] when discharge measurements were available. The time integral of mass fluxes equals the recovered tracer masses, and the ratio of mass flux to total tracer mass gives a PDF of tracer travel times along the transport distance. Mass fluxes were normalised using the total mass of tracer recovered during the measurement, such that the integral of the PDF is unity. The travel time PDF allows conclusion on the transport regime along/through its moments, e.g. mean travel time and travel time variance, cf. Eqs. (3) and (4). Trapezoidal rule integration was used for moment estimation as suggested by Haas (1996). To allow for a consistent determination of moments and comparability between experiments, the travel time PDF was constructed from tracer BTCs truncated to 0.1% of maximum concentration in the tailing.

Specific process representations of the travel time PDF can be derived for respective boundary and initial conditions (Jury and Roth, 1990). The most commonly used process model for solute movement in porous media is the convection-dispersion equation (CDE). A compilation of transfer function representations for the CDE is given by van Genuchten and Alves (1982). The CDE describes solute transport in the well-mixed case such that each solute molecule experiences the complete range of transport velocities during the transport process. Linear adsorption is the simplest model of an adsorbing tracer, assuming instantaneous equilibrium between solute concentrations in the adsorbed and liquid phase. Transport of a sorbing solute is then retarded, compared to a non-sorbing solute, by a constant retardation factor  $R$ . The corresponding

2972

derstand how heterogeneities in rainfall and subsurface structures translate into BTCs of tracer experiments.

## 5 Summary and conclusions

Subsurface stormflow in response to heavy rainfall has been studied at a forested hillslope in the Austrian Alps using a combination of dye staining at the plot scale with rainfall simulations and tracer tests at the hillslope scale. Steep forested slopes constitute especially challenging environments for experimental work. For example, slope topography only allowed covering parts of the experimental area with rainfall simulations. Nevertheless, this setup was sufficient to produce subsurface flow within the hillslope and maintain quasi-steady state flow rates at a spring and a cut-bank downslope.

Salts (NaCl, NaBr) and fluorescent dyes (uranine, sulforhodamine G) applied at the soil surface were suitable for tracing subsurface flow over distances of up to 32.4 and 44.2 m, respectively. Despite the fine-textured soils, tracer breakthrough was fast in all experiments, with breakthrough velocities ranging from  $1.0 \times 10^{-2}$  to  $2.0 \times 10^{-3} \text{ m s}^{-1}$ . Breakthrough curves were measured in situ with high temporal resolution, which proved to be especially advantageous in the case of highly dynamic fluorescence tracers in transient flow conditions under natural rainfall. Under these circumstances salts were not appropriate as tracers, because estimations of concentrations via electrical conductivity and with ion chromatography were precluded due to strong dilution by rainwater. However, under simulated rainfall the breakthrough of salt tracers was captured well with electrical conductivity readings, and nearly complete recovery of tracer mass was achieved. In contrast, we found very low recovery rates of the fluorescent dyes during the hillslope experiments. Uranine tracer tests with an undisturbed soil block (0.35 m depth) from the study area yielded similar low recovery rates. Although the reasons were not definitively clarified by our experiments, the apparent loss of tracer was evidently caused by interactions of dye and soil material in the top-most soil lay-

2987

ers. This finding implies that tracers need to be selected carefully and checked for interactions with the specific soil material. From the soil block results we conclude that the hillslope scale BTC of the fluorochromes reflects the transport behaviour of the mobile tracer fraction only. Dye staining revealed that infiltration was quite uniform down to a depth of 0.15 m, and that percolation below was dominated by preferential flow along soil pipes, desiccation cracks and the bedrock surface. The mobile tracer fraction thus resembles the fast infiltration and subsurface flow processes which are dominating subsurface stormflow characteristics at this site.

The tracer BTCs obtained under steady-state conditions were reproduced reasonably well by a one-dimensional convection dispersion model. Despite the relatively large transport distances of the tracer experiments, the resulting Peclet numbers were low, which implies that Lagrangian transport distances for this highly dispersive medium are in the range of tens of metres. Furthermore, the steady-state BTCs offer only a limited view on the flow processes, and any lumped-process representation is not necessarily applicable for predicting subsurface transport under different conditions (rainfall input, soil moisture state) or along different flow paths. This conclusion is corroborated by the tracer BTCs obtained under transient natural rainfall conditions, which interestingly were closely related to rainfall and discharge dynamics. Transport paths and breakthrough velocities were strongly dependent on the application locations, the heterogeneity of rainfall and the respective spatial arrangement of flow paths.

Preferential flow and transport at the hillslope scale lead to very inefficient mixing that exacerbates and utilisation of the widely used CDE approach. Transfer functions as lumped representations of transport processes are conditional on, and thus limited to, the range of experimental conditions. The setup of a numerical model to simulate this fast responding system, which is intended for a consecutive study, will require detailed representations of subsurface structures and heterogeneities. Nevertheless, the experimental results obtained in this study demonstrates both the potential and the limitations of applied tracers for exploring site-specific characteristics of subsurface stormflow processes at the hillslope scale, and will provide an integral part of the data

fluorescence  
tracers

2988

basis for future applications in hillslope hydrological modelling at this site.

*Acknowledgements.* This work has been funded by Deutsche Forschungsgemeinschaft (DFG For 581). Thanks are due to Niko Bornemann, Mareike Eichler and Erik Sommerer for their motivated assistance during field work, to Wolfgang Peter for providing technical support, and to Jim Freer for helpful comments on an earlier version of the manuscript.

## References

- Amoozegar, A.: A compact constant-head permeameter for measuring saturated hydraulic conductivity of the vadose zone, *Soil Sci. Soc. Am. J.*, 53, 1356–1361, 1989. 2967
- Anderson, A. E., Weiler, M., Alila, Y., and Hudson, R. O.: Dye staining and excavation of a lateral preferential flow network, *Hydrol. Earth Syst. Sci. Discuss.*, 5, 1043–1065, 2008, <http://www.hydrol-earth-syst-sci-discuss.net/5/1043/2008/>. 2965, 2979
- Binley, A., Henry-Poulter, S., and Shaw, B.: Examination of solute transport in an undisturbed soil column using electrical resistance tomography, *Water Resour. Res.*, 32, 763–769, 1996. 2965, 2982
- Blume, T., Zehe, E., and Bronstert, A.: Investigation of runoff generation in a pristine, poorly gauged catchment in the Chilean Andes II: Qualitative and quantitative use of tracers at three spatial scales, *Hydrol. Process.*, 22, 3676–3688, doi:10.1002/hyp.6970, 2008. 2965, 2971
- Bonell, M.: Progress in the understanding of runoff generation dynamics in forests, *J. Hydrol.*, 150, 217–275, 1993. 2962
- Bouma, J. and Dekker, L. W.: A method for measuring the vertical and horizontal Ksat of clay soils with macropores, *Soil Sci. Soc. Am. J.*, 45, 662–663, 1981. 2968
- Brusseau, M. L., Hu, Q., and Srivastava, R.: Using flow interruption to identify factors causing nonideal contaminant transport, *J. Contam. Hydrol.*, 24, 205–219, 1997. 2968, 2983, 2985
- Chua, L. H. C., Robertson, A. P., Yee, W. K., Shuy, E. B., Lo, E. Y. M., Lim, T. T., and Tan, S. K.: Use of Fluorescein as a Ground Water Tracer in Brackish Water Aquifers, *Ground Water*, 45, 85–88, 2007. 2982
- Das, B. S., Wraith, J. M., Kluitenberg, G. J., Langner, H. M., Shouse, P. J., and Inskeep, W. P.: Evaluation of mass recovery impacts on transport parameters using least-squares optimization and moment analysis, *Soil Sci. Soc. Am. J.*, 69, 1209–1216, 2005. 2973, 2984

2989

- Deeks, L. K., Bengough, A. G., Stutter, M. I., Young, I. M., and Zhang, X. X.: Characterisation of flow paths and saturated conductivity in a soil block in relation to chloride breakthrough, *J. Hydrol.*, 348, 431–441, 2008. 2965
- Divine, C. E. and McDonnell, J. J.: The future of applied tracers in hydrogeology, *Hydrogeol. J.*, 13, 255–258, 2005. 2964
- Flury, M. and Wai, N. N.: Dyes as tracers for vadose zone hydrology, *Rev. Geophys.*, 41, 1002, doi:10.1029/2001RG000109, 2003. 2964
- Flury, M., Flüher, H., Jury, W. A., and Leuenberger, J.: Susceptibility of Soils to Preferential Flow of Water – a Field-Study, *Water Resour. Res.*, 30, 1945–1954, 1994. 2965
- Freer, J., McDonnell, J. J., Beven, K. J., Peters, N. E., Burns, D. A., Hooper, R. P., Aulenbach, B., and Kendall, C.: The role of bedrock topography on subsurface storm flow, *Water Resour. Res.*, 38, 1269, doi:10.1029/2001WR000872, 2002. 2979
- Germann, P. F.: Length scales of convection-dispersion approaches to flow and transport in porous media, *J. Contam. Hydrol.*, 7, 39–49, 1991. 2986
- Haas, C. N.: Moment analysis of tracer experiments, *J. Environ. Eng.-ASCE*, 122, 1121–1130, 1996. 2972
- Henderson, D. E., Reeves, A. D., Beven, K. J., and Chappell, N. A.: Flow separation in undisturbed soil using multiple anionic tracers .2. Steady-state core-scale rainfall and return flows and determination of dispersion parameters, *Hydrol. Process.*, 10, 1451–1465, 1996. 2965
- Hornberger, G. M., Beven, K. J., and Germann, P. F.: Inferences about solute transport in macroporous forest soils from time series models, *Geoderma*, 46, 249–262, doi:10.1016/0016-7061(90)90018-5, 1990. 2965
- Jensen, K. H., Destouni, G., and Sassner, M.: Advection-dispersion analysis of solute transport in undisturbed soil monoliths, *Ground Water*, 34, 1090–1097, 1996. 2965, 2986
- Joerin, C., Beven, K. J., Musy, A., and Talamba, D.: Study of Hydrol. Process. by the combination of environmental tracing and hill slope measurements: application on the Haute-Mentue catchment, *Hydrol. Process.*, 19, 3127–3145, 2005. 2964, 2980
- Jones, J. A. A. and Connelly, L. J.: A semi-distributed simulation model for natural pipeflow, *J. Hydrol.*, 262, 28–49, 2002. 2963
- Jury, W. A.: Simulation of Solute Transport Using a Transfer-Function Model, *Water Resour. Res.*, 18, 363–368, 1982. 2985
- Jury, W. A. and Roth, K.: *Transfer Functions and Solute Movement Through Soil*, Birkhäuser Verlag, Basel, Switzerland, 235 pp., 1990. 2971, 2972

hydrological  
processes

- Wilson, G. V., Jardine, P. M., Luxmoore, R. J., Zelazny, L. W., Lietzke, D. A., and Todd, D. E.: Hydrogeochemical processes controlling subsurface transport from an upper subcatchment of Walker Branch watershed during storm events. 1. Hydrologic transport processes, J. Hydrol., 123, 297–316, 1991. 2981
- 5 Zehe, E. and Flüher, H.: Slope scale variation of flow patterns in soil profiles, J. Hydrol., 247, 116–132, 2001a. 2965, 2969, 2971
- Zehe, E. and Flüher, H.: Preferential transport of isoproturon at a plot scale and a field scale tile-drained site, J. Hydrol., 247, 100–115, 2001b. 2965, 2981

2995

**Table 1.** Details of tracer experiments at the hillslope scale and with the soil block.

Experiment identifier and employed tracers	Location of application (application area / total plot area)	Applied tracer mass, volume of solution
<i>Soil block</i>		
Uranine 1	Soil block (0.0506 m <sup>2</sup> )	0.4 g in 0.1 l
Uranine 2		0.25 g in 0.1 l
Salt 1: NaCl		25 g in 0.1 l
Salt 2: NaCl		5 g in 0.1 l
<i>Hillslope scale: Natural rainfall</i>		
Uranine/ Sulforhodamine G	Plot IV (4 m <sup>2</sup> /20 m <sup>2</sup> )	2.1 g/4.2 g in 4.5 l
NaCl	Plot IIIa (0.24 m <sup>2</sup> )	3000.0 g in 10 l
NaBr	Plot II (4 m <sup>2</sup> /29 m <sup>2</sup> )	772.72 g in 10 l
Uranine/ Sulforhodamine G	Plot I (9 m <sup>2</sup> /33 m <sup>2</sup> )	0.4 g/0.8 g in 0.9 l
<i>Hillslope scale: steady-state</i>		
Uranine 1	Plot IIIb (4 m <sup>2</sup> /33 m <sup>2</sup> )	2.5 g in 2.5 l
Uranine 2	Plot IIIb (4 m <sup>2</sup> /33 m <sup>2</sup> )	2.5 g in 2.5 l
Salt 1: NaCl	Plot I (4 m <sup>2</sup> /15 m <sup>2</sup> )	2500.0 g in 15 l
Salt 2: NaCl	Plot II (4 m <sup>2</sup> /28 m <sup>2</sup> )	2277.3 g in 15 l

add lines to improve readability

2996



**Table 2.** First hillslope tracer experiment – Correlations of tracer BTCs, rainfall and spring discharge: Pearson product-moment correlation coefficients  $r$  and time lags for complete time series and periods during and after rainfall simulations, respectively. Time lags are positive if column variables are preceding.

	effective (natural + applied) rainfall		natural rainfall		spring discharge	
	$r$	time lag	$r$	time lag	$r$	time lag
<i>complete series</i>						
uranine	0.49	2400	0.29	2520	0.43	120
sulforhodamine G	0.67	240	0.66	240	0.58	-2400
spring	0.24	2520	0.54	2640		
<i>during simulation</i>						
uranine	0.11	2400	0.00	2400	-0.62	120
sulforhodamine G	0.43	240	0.33	240	-0.05	-2400
spring	0.04	2520	0.70	5400		
<i>after simulation</i>						
uranine	0.37	2400	0.37	2400	0.64	120
sulforhodamine G	0.75	240	0.75	240	0.72	-2400
spring	0.55	2520	0.55	2520		

add lines to improve readability

2997

**Table 3.** Soil block experiment and second hillslope experiment: Velocities corresponding to time of first breakthrough, peak of tracers and mean travel time (first moment of travel time PDF), travel time variance (second central moment) and tracer recovery (% mass applied).

	Distance [m]	Breakthrough velocity [m s <sup>-1</sup> ]	Peak velocity [m s <sup>-1</sup> ]	Mean travel velocity [m s <sup>-1</sup> ]	Travel time variance [s <sup>2</sup> ]	Recovery (corrected BTC) [%]
<i>Soil block</i>						
Uranine 1	0.35	$1.17 \times 10^{-3}$	$1.72 \times 10^{-4}$	$9.68 \times 10^{-6}$	$2.77 \times 10^9$	22.02
Uranine 2	0.35	$2.33 \times 10^{-3}$	$4.32 \times 10^{-4}$	$8.49 \times 10^{-5}$	$1.11 \times 10^7$	5.18 (6.07)
Salt 1	0.35	$5.83 \times 10^{-3}$	$1.46 \times 10^{-3}$	$2.07 \times 10^{-4}$	$6.81 \times 10^6$	89.23
Salt 2	0.35	$2.92 \times 10^{-3}$	$1.17 \times 10^{-3}$	$7.22 \times 10^{-4}$	$6.48 \times 10^4$	81.50
<i>Hillslope scale: Cut-bank</i>						
Uranine 1	28.7	$1.04 \times 10^{-2}$	$3.95 \times 10^{-3}$	$9.65 \times 10^{-4}$	$5.40 \times 10^8$	2.9 (2.93)
Uranine 2	28.7	$7.97 \times 10^{-3}$	$3.80 \times 10^{-3}$	$1.16 \times 10^{-3}$	$2.37 \times 10^8$	7.87 (14.18)
Salt 1	8.2	$1.37 \times 10^{-2}$	$2.63 \times 10^{-3}$	$5.93 \times 10^{-4}$	$2.20 \times 10^8$	94.18
Salt 2	16.9	$8.54 \times 10^{-3}$	$1.18 \times 10^{-3}$	$7.51 \times 10^{-4}$	$1.37 \times 10^8$	32.1
<i>Hillslope scale: Spring</i>						
Uranine 1	44.2	$2.73 \times 10^{-2}$	$1.62 \times 10^{-3}$	$1.15 \times 10^{-3}$	$6.75 \times 10^8$	0.45
Uranine 2	44.2	$3.78 \times 10^{-3}$	$3.42 \times 10^{-4}$	$1.32 \times 10^{-3}$	$2.10 \times 10^8$	0.86
Salt 1	23.7	$4.49 \times 10^{-3}$	$2.18 \times 10^{-3}$	$5.18 \times 10^{-4}$	$9.66 \times 10^8$	7.45
Salt 2	32.4	$2.07 \times 10^{-3}$	$8.71 \times 10^{-4}$	$6.48 \times 10^{-4}$	$4.47 \times 10^8$	3.46

add lines to improve readability

Salt 1 and 2 : NaCl ?

2998

**Table 4.** Results from fitting of CDE parameters for soil block experiment and second hillslope experiment:  $R$ ,  $V$  and  $D$  (fixed values are printed italic),  $r^2$ , coefficient of determination of regression of observed against predicted data, and corresponding Peclet numbers  $Pe$ .

	Distance [m]	$R$ [-]	$V$ [ $m\ s^{-1}$ ]	$D$ [ $m^2\ s^{-1}$ ]	$r^2$ [-]	$Pe$ [-]
<i>Soil block</i>						
Salt 1	0.35	1	$5.34 \times 10^{-4}$	$7.21 \times 10^{-5}$	0.91	2.59
Salt 2	0.35	1	$6.84 \times 10^{-4}$	$4.05 \times 10^{-5}$	0.76	5.92
Uranine 2	0.35	28.5	$6.84 \times 10^{-4}$	$7.75 \times 10^{-4}$	0.94	0.31
Uranine 1	0.35	28.5	$1.24 \times 10^{-4}$	$2.36 \times 10^{-4}$	0.97	0.18
<i>Hillslope scale: Cut-bank</i>						
Uranine 1	28.7	1	$8.70 \times 10^{-4}$	$1.57 \times 10^{-2}$	0.92	1.59
		28.5	$2.48 \times 10^{-2}$	$4.47 \times 10^{-1}$	0.92	1.59
		0.63	$5.55 \times 10^{-4}$	$9.92 \times 10^{-3}$	0.92	1.60
Uranine 2	28.7	1	$9.82 \times 10^{-4}$	$1.22 \times 10^{-2}$	0.85	2.31
		28.5	$2.80 \times 10^{-2}$	$3.47 \times 10^{-1}$	0.85	2.31
		0.60	$5.91 \times 10^{-4}$	$7.33 \times 10^{-3}$	0.85	2.31
Salt 1	8.2	1	$5.55 \times 10^{-4}$	$4.13 \times 10^{-3}$	0.95	1.10
Salt 2	16.9	1	$5.91 \times 10^{-4}$	$2.96 \times 10^{-3}$	0.80	3.38
<i>Hillslope scale: Spring</i>						
Uranine 1	44.2	1	$1.28 \times 10^{-3}$	$9.71 \times 10^{-3}$	0.49	5.83
		28.5	$3.65 \times 10^{-2}$	$2.77 \times 10^{-1}$	0.49	5.83
Uranine 2	44.2	1	$1.18 \times 10^{-3}$	$8.41 \times 10^{-3}$	0.86	6.22
		28.5	$3.37 \times 10^{-2}$	$2.40 \times 10^{-1}$	0.86	6.22
Salt 1	23.7	1	$4.56 \times 10^{-4}$	$4.59 \times 10^{-3}$	0.94	2.35
Salt 2	32.4	1	$6.15 \times 10^{-4}$	$2.69 \times 10^{-3}$	0.85	7.41

add lines to improve readability

2999

Salt 1 + 2 : NaCl ?

Use same style as in caption

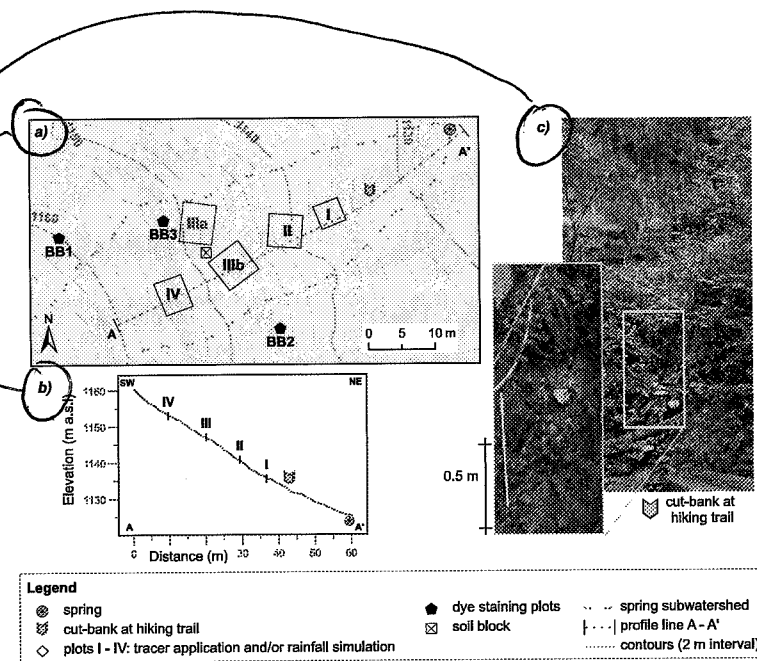


**Fig. 1.** (a) Map of experimental area and setup of hillslope tracer experiments. (b) Topographic cross section along A-A' in inset a). (c) Photographs of cut-bank where a hiking trail crosses the slope and exfiltration occurs after rainfall events. Fluorescence tracers were measured in the outflow at this location and at the spring.

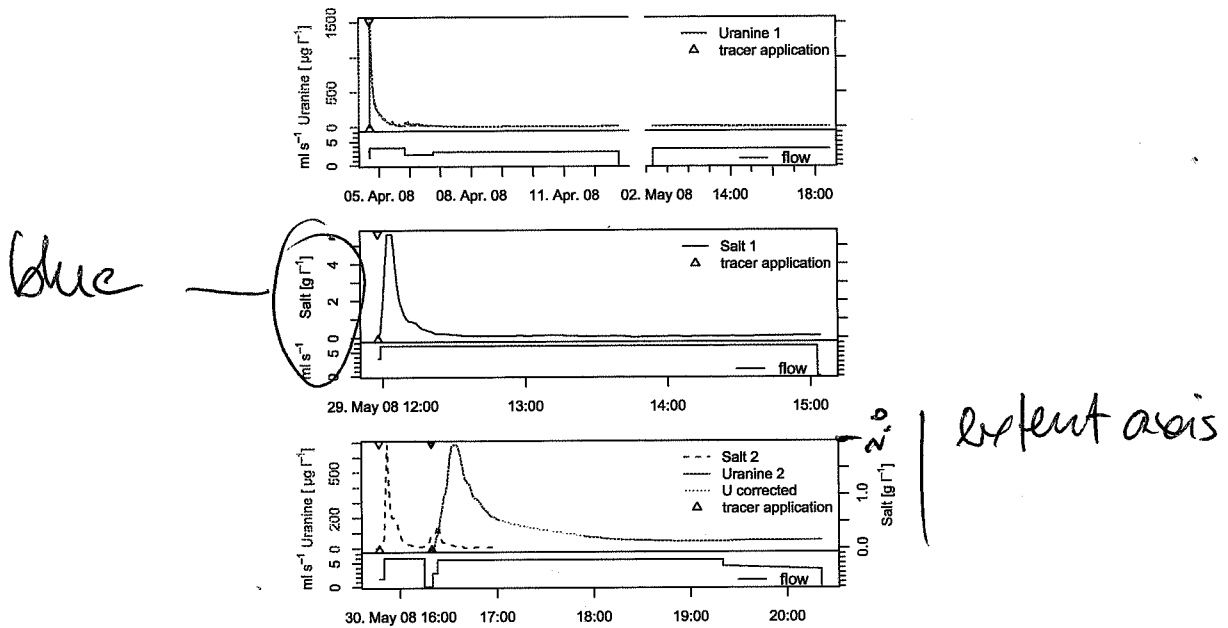


**Fig. 2.** Soil block experiments: Tracer breakthrough curves (uranine and NaCl) and water flows of three subsequent runs (times are Central European Time). The soilblock was flushed with tracer free water before each run, and inflow was interrupted for 19 days during the first run. A gap in the second uranine BTC (lower panel) was corrected using spline interpolation for a second estimate of tracer recovery (Table 3).

3001

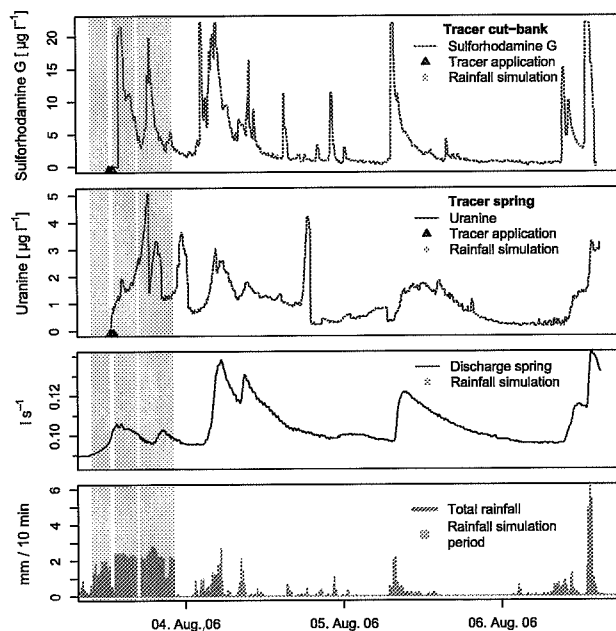


**Fig. 3.** First hillslope experiment under natural rainfall conditions: Tracer breakthrough curves (sulfurhodamine G in outflow at cut-bank, uranine in spring discharge), spring discharge and total rainfall (from top to bottom). Grey shading marks the rainfall simulation period.

3002

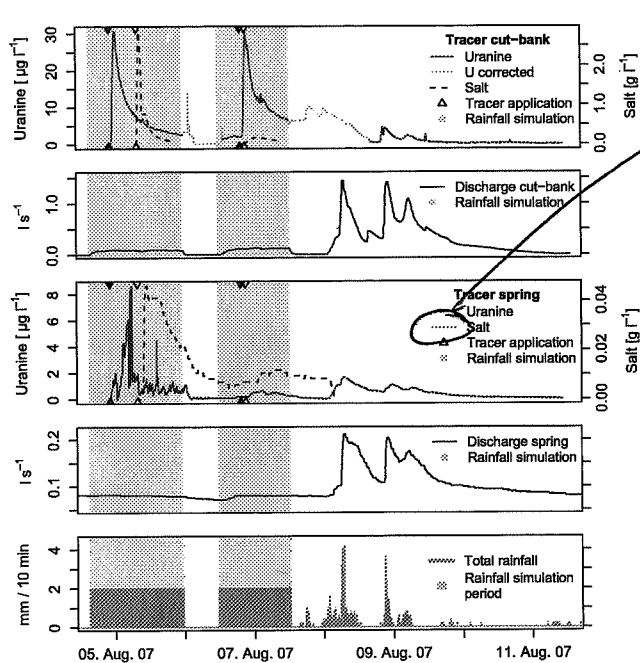


**Fig. 4.** Second hillslope experiment under steady flow conditions: Tracer breakthrough curves for uranine and NaCl at the cut-bank, discharge at the cut-bank, tracer BTCs of uranine and NaCl in spring discharge, discharge at spring, and total rainfall (from top to bottom). Grey shading marks the rainfall simulation period and were excluded from further analyses; the manually corrected data were used for a second estimate of recovery (Table 3).

3003

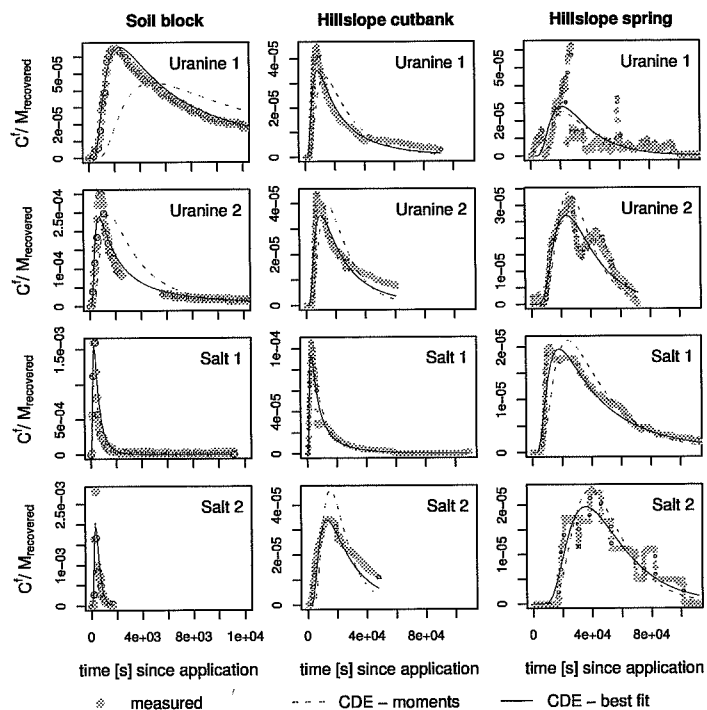


**Fig. 5.** Travel time probability functions of soil block experiments and second hillslope tracer experiments with uranine and NaCl. The PDFs were derived from the measured breakthrough curves and modelled with the convection-dispersion equation, parameterised either with the moments of the measured BTC or fitted parameters.

3004

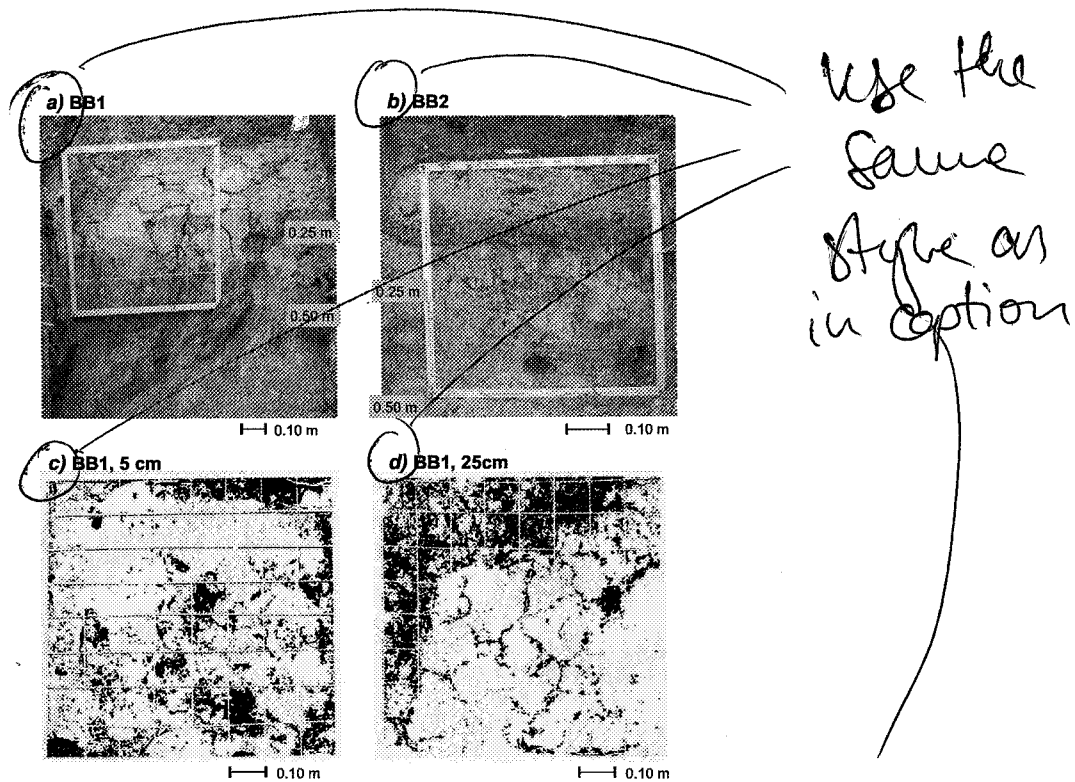


**Fig. 6.** Dye staining experiments (for location cf. Fig. 1): **(a)** Photograph of soil profile BB1 showing cracks and dye-stained bedrock (horizontal section in 0.25 m depth and vertical section from 0.25–0.50 m). **(b)** Photograph of soil profile BB2 showing pipes of several cm in the topsoil and above bedrock (horizontal section in 0.10 m depth and vertical section from 0.10–0.50 m). **(c), (d):** Binarized horizontal cross-sections (0.05 and 0.25 cm below surface) of soil profile BB1 showing stained areas in dark.

3005

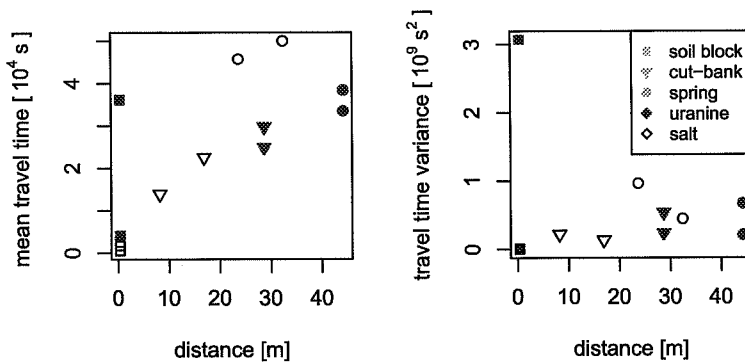


**Fig. 7.** Soil block and second hillslope tracer experiment: Mean travel time (first moment; left) and travel time variance (second central moment; right) of travel time PDF vs. travel distance (individual experiments indicated by combination of symbol shape and filling).

3006